Available online at www.sciencedirect.com

ScienceDirect

Ceramics International 40 (2014) 14769–14779

CERAMICS INTERNATIONAL

www.elsevier.com/locate/ceramint

Spectroscopic and thermal techniques for the characterization of the first millennium AD potteries from Kuriki-Turkey

Murat Bayazit[a,*], Iskender Işık[b], Ali Issi[b], Elif Genç[c]

[a]Department of Ceramics, Faculty of Fine Arts, Batman University, Central Campus, 72060 Batman, Turkey
[b]Department of Materials Science & Engineering, Faculty of Engineering, Dumlupınar University, Evliya Çelebi Campus, 43100 Kütahya, Turkey
[c]Department of Archeology, Faculty of Science and Letters, Çukurova University, 01330 Adana, Turkey

Received 23 May 2014; received in revised form 11 June 2014; accepted 12 June 2014
Available online 19 June 2014

Abstract

This study focuses on the archaeometrical characterization of the potteries belonging to the First Millennium AD from the Kuriki Mound using thermal, mineralogical, microscopic and spectroscopic techniques. The excavation area takes place at the intersection point of the Tigris River and the Batman Creek near the village of Oymataş in Batman city (Turkey). Since this region is located at Upper Mesopotamia, it is one of the important ancient sites in southeastern Anatolia and represents the cultural heritage of the civilizations that lived there. In the framework of the present study, thermogravimetric–differential thermal analysis (TG–DTA) and ceramic petrography were employed to characterize the potsherds. X-ray diffraction (XRD), scanning electron microscopy (SEM) and energy dispersive spectroscopy (EDS), micro-Raman spectroscopy and colorimetric analyses were also performed as complementary techniques. The results showed that the mineralogical composition of the pottery consists mainly of quartz, feldspar and plagioclase. Clay minerals (mainly illite) and organic materials were identified as the minor phases, while carbonated materials (mainly calcite) were seen as major and minor phases in different samples. Iron minerals were also detected by XRD and micro-Raman analyses. A relatively low vitrification degree along with the poor sinterization behavior defined in SEM/EDX analysis and the absence of any prominent endothermic or exothermic effects on DTA curves up to 1000–1100 °C suggested that the firing temperature of the potteries did not exceed this range. The main reason for such characteristics is thought to be a non-advanced firing technique.
© 2014 Elsevier Ltd and Techna Group S.r.l. All rights reserved.

Keywords: Ancient Turkish pottery; Upper Mesopotamia; Southern Anatolia; Kuriki (Turkey)

1. Introduction

Being one of the most abundant and stable products, ceramic wares have a great importance in terms of enlightening the history of human [1]. Especially identification of the production techniques of ancient potteries provides a substantial knowledge with respect to the technological aspects of the past civilizations [2]. The initial raw materials, coloring agents, temper materials and other additives for various purposes, and also the firing conditions such as maximum firing temperature, soaking time and firing atmosphere, all of which depend on the firing technique (pit, bonfire or kiln firing), allow us to estimate the status of the human being in ancient times [3]. In last decades archaeometry, which gathers various branches of the science like archeology, engineering sciences, art history, physics, chemistry, biology etc., is widely exercised in all over the world much more than what is done for preservation and conservation of cultural heritages.

Since the Kuriki Mound (Fig. 1) is located in Upper Mesopotamia, the data obtained within the archaeometrical researches carried out both in this region and the vicinity will provide a substantial knowledge of social and cultural aspects of the territory. With this intention, the potsherds were investigated using thermal, mineralogical, microscopic and spectroscopic techniques. Thermogravimetric–differential thermal analysis (TG–DTA) was performed to observe the thermal behaviors of the samples and to predict the maximum firing temperatures. Petrographic analysis was applied using polarized-light optical

*Corresponding author. Tel.: +90 488 2173500; fax: +90 488 2173601.
E-mail address: m.bayazit@hotmail.com (M. Bayazit).

http://dx.doi.org/10.1016/j.ceramint.2014.06.068
0272-8842/© 2014 Elsevier Ltd and Techna Group S.r.l. All rights reserved.

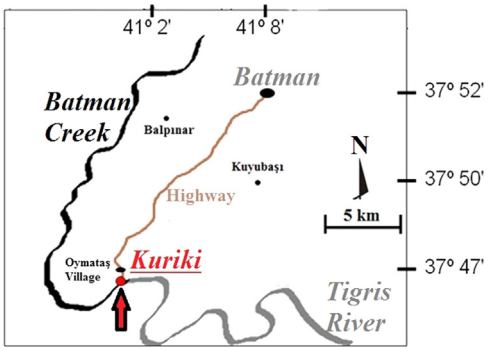


Fig. 1. Representative image of the location of Kuriki.

microscopy to define the starting raw materials of the ceramics. Other methods used as complementary techniques in this work were: X-ray diffraction (XRD) for identification of mineral/phases, scanning electron microscopy (SEM) and energy dispersive spectroscopy (EDS) for microstructural and microchemical properties, micro-Raman spectroscopy for determination of mineral compositions (particularly the coloring agents) and colorimetric analysis for measuring of the colors of the potsherds.

2. Sampling and experimental

2.1. Samples

In the present work 14 representative potsherds (Fig. 2) of the 1st millennium AD from Kuriki (Turkey) were studied. The samples were selected from the first archeological settlement layer which comes after the Part-Roma period (end of the 1st millennium BC and the beginning of the 1st millennium AD). The fundamental criteria in selection process of the potsherds was to find the most appropriate fragments which are able to represent the whole of the other similar products found in the same archeological settlement layer of the mound. With this aim, the sampling group consisted of the potsherds including handle, rim, neck and edge of the wares with the red, brown, buff and gray colors. By macro observation of the samples it was seen that the samples of S2, S3, S6, S7, S9 and S12 contain traces of wheel-made production. It was also observed that some of the samples (S4, S5, S7, S8, S11 and S14) have red-brown margin with black-gray core implying a sandwich structure probably indicating a variation of atmosphere conditions from reducing to oxidizing in the last step of the firing. It was also seen that the samples of S1, S7, S8, S11 and S14 have elongated signs on their surfaces. The samples of S4 and S11 have smoke stains indicating traces of an over-burned body or probably of use as cooking ceramics. A thin off-white layer was observed on the surface of the sample S13, probably indicative of a slip layer/glaze-like structure. Finally the samples do not include any apparent decoration or figure which is attributed to a purpose of simple use.

2.2. Experimental

After the purification process of the potsherds, an agate mortar was used to grind the samples so as to be analyzed by thermal gravimetric-differential thermal analysis (TG–DTA) and X-ray diffraction (XRD) techniques. Netzsch STA 449F3 instrument supported with Netzsch Proteus software was used for TG–DTA analyses. A heating rate of 10 °C/min was performed in oxidative atmosphere from room temperature to 1100 °C. Leica Research Polarizing Microscope (DMLP Model) with top and bottom illumination was performed for the petrographic investigations in which the thin sections of the samples were used in order to observe all outer and inner layers. Leica DFC280 digital camera (single and double nicol) with × 25 magnification was used to obtain the images. Leica Qwin digital imaging program and Point Counting method were used in assessment process of the results of petrographic analysis.

Colorimetric analysis of the potsherds was performed using a portable colorimeter with ColorQA Pro System III program. For the identification of the shades CEI (Commission Internationale de L'Eclairage) L-a-b color system was used. Determination of mineral/phase content of the samples was carried out using Rigaku Miniflex powder diffractometer with Cu Kα radiation. A goniometer speed of 2°/min and the scanning range of 2–70° 2θ were used to obtain the XRD patterns. Jade was used as the software in assessment process of the XRD results. The microstructural and microchemical aspects of the representative potsherds were investigated using the Zeiss Supra 50VP SEM which also includes the EDS detector of Oxford Instruments INCA Energy. Raman spectra of the representative samples were obtained using Horiba Jobin Yvon LabRam confocal Raman spectrograph equipped with the Olympus BX41 microscope and Peltier cooling CCD (1024 × 256 pixels) detector. He/Ne laser (632.8 nm) with a power limit of 700 μW was used for the Raman excitation in order to preserve the sample. At least 20 spectra were recorded for each representative sample. Raman PCI model video camera was used to obtain the microscopic images of the samples.

3. Results

3.1. Mineralogical analyses

3.1.1. Ceramic petrography

Thin sections of the samples were prepared for the petrographic micro morphological investigations of the potsherds and then were observed under the polarizing microscope with top and bottom illumination. Table 1 shows the total aggregate amount, grog content and mineralogical assemblages together with the clay and rock types identified in the potsherds.

According to the results obtained by the ceramic petrography it was seen that the illitic clay type has particularly been used in manufacture of the ceramics. Little smectitic and kaolinitic clay types were identified in few samples (illitic + smectitic: S2; smectitic: S10; illitic + kaolinitic: S14). Opaque minerals (hematite, magnetite) and quartz were present in all samples. Plagioclase, chert and sericite were identified in most of the samples. Biotite, chalcedony, muscovite and quartzite

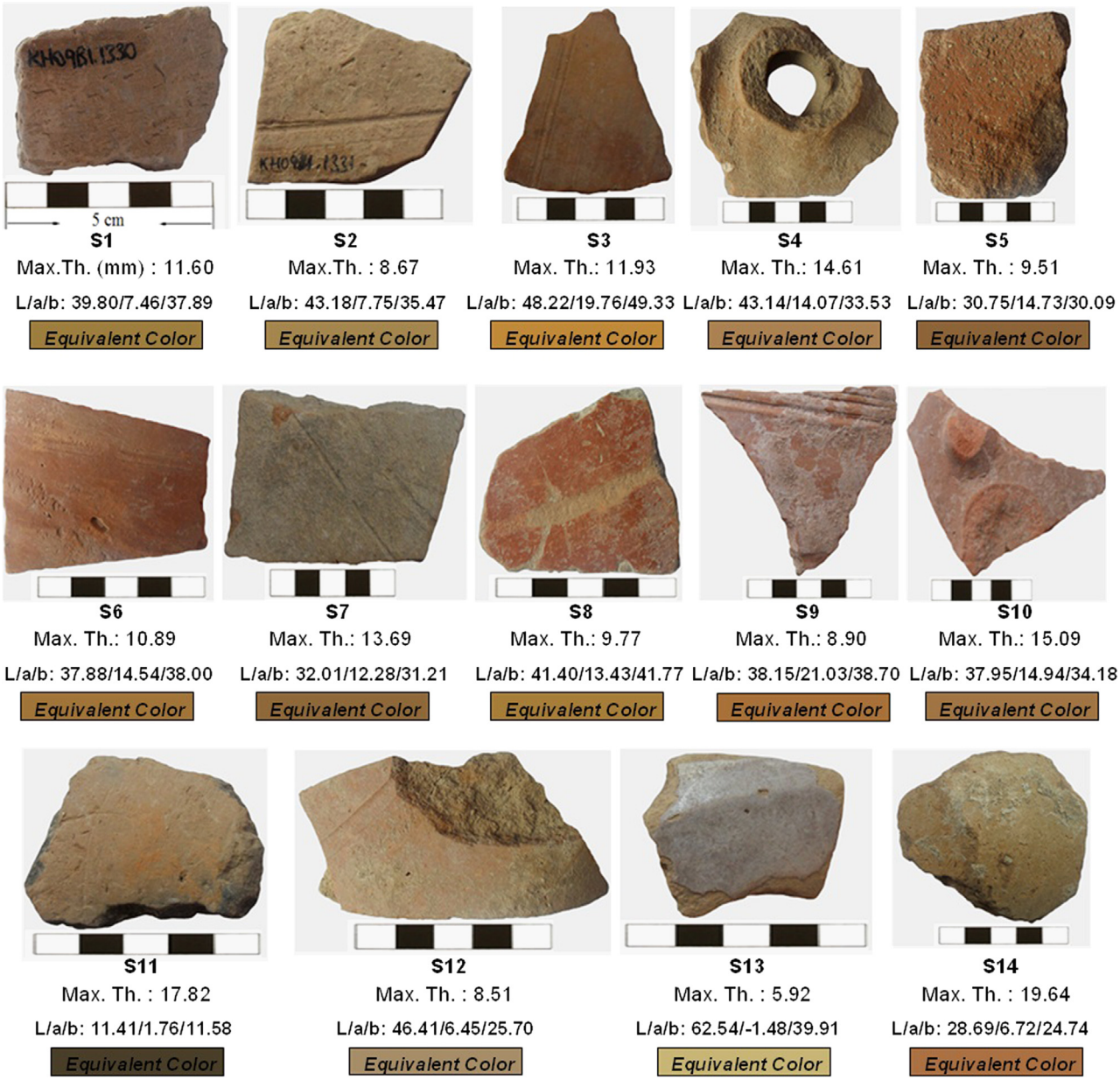


Fig. 2. The representative images of the studied samples (Max. Th.: Maximum Thickness). The equivalent colors were assigned through the values of L^*/ a^{**}/ b^{***}. *The darkness/lightness values of "L" changes from 0 (white) to 100 (black). **The positive values of "a" (from 0 to 60) represents the red intensity and the negative values of "a" (from 0 and to −60) represents the green intensity. ***The yellow intensity is represented by the positive values of "b" (from 0 to 60) and the blue intensity is represented by the negative values of "b" from (0 to −60) (for interpretation of the references to color in this figure legend, the reader is referred to the web version of this article).

were the less abundant minerals found in the potsherds. Basalt (effusive igneous rock formation) and limestone were assigned as the rock types which are thought to be the main sources for the minerals specified in the ceramic fabrics. Total aggregate content of the samples is relatively high and changes between 13 and 58 vol% (in cross-sectional area) probably indicating a poor selection of the starting raw materials. Some grog fragments were also detected in cross-sectional areas of almost half of the samples (S1, S3, S6, S8, S9 and S11) suggesting a possible recycling process of the worn-out and/or faulty products (Fig. 3(a)).

From the microphotographs of the representative samples we may classify the samples into two groups according to the size and distribution of the grains forming the ceramic fabrics. The first group possesses an inhomogeneous paste with high non-plastic material/matrix ratio and with relatively coarse grains advising a poor refining of the raw materials (Fig. 3(b)). The second group consists of relatively fine grains which are well-dispersed into the matrix of the sample (Fig. 4(a)). It was also seen that some of the potsherds have color and contrast transitions suggesting that they were presumably subjected to an uneven firing process due to lack of homogeneity of

temperature distribution (Fig. 4(b)). These directive results will provide a basis for further analyses especially for XRD.

3.1.2. X-ray diffraction

Identification of mineral/phase contents of the ancient ceramic wares provides a substantial knowledge which will allow revealing the production techniques and estimating the firing conditions such as maximum temperature reached, firing atmosphere and the firing techniques used by the potters [4]. Depending mainly on the composition of starting materials, interactions between grains and clay matrix would be seen through a heat treatment in production of clay based traditional ceramics [5]. For instance, the firing minerals such as gehlenite ($Ca_2Al_2SiO_7$), anorthite ($CaAl_2Si_2O_8$) and pyroxene (diopside [Ca(Mg,Al) $(Si,Al)_2O_6$], augite [$Ca(Mg,Fe)Si_2O_6$]) occur due to the reaction between CaO derived from the carbonates decomposition and the amorphous material from the destruction of the clay mineral crystalline structure [5,6]. Gehlenite and anorthite-pyroxene were distinctly identified in the XRD spectra of the samples of S2 and S13, respectively, suggesting firing temperatures from a minimum of 800 °C to 900 °C.

Table 1
Ceramic petrography results of the samples.

Sample code	Aggregate (vol%)	Clay type	Mineral[a]	Rock[b] and Grog (%)
S1	31	Illitic	Q,Pl,Sr,Op	Grog (%1,5)
S2	18	Illitic + Smectitic	Q,Pl,Ch,Bi,Op	–
S3	31	Illitic	Q,Pl,Sr,Op	Grog (%1,5)
S4	43	Illitic	Q,Pl,Ch,Bi,Op,Ms	L
S5	58	Illitic	Q,Pl,Ch,Op	B
S6	31	Illitic	Q,Pl,Sr,Op	Grog (%1,5)
S7	13	Illitic	Q,Pl,Ch,Op,	–
S8	31	Illitic	Q,Pl,Sr,Op	Grog (%1,5)
S9	31	Illitic	Q,Pl,Sr,Op	Grog (%1,5)
S10	29	Smectitic	Q,Ch,Ms,Qs,Bi,Op	–
S11	31	Illitic	Q,Pl,Sr,Op	Grog (%1,5)
S12	13	Illitic	Q,Ch,Bi,Op	–
S13	43	Illitic	Q,Pl,Ch,Bi,Op,Ms,	L
S14	23	Illitic + Kaolinitic	Q,Pl,Ch,Op,Cy	–

–: not defined

[a] **Bi:** biotite, **Ch:** chert, **Cy:** chalcedony, **Ms:** muscovite, **Op:** opaque minerals (e.g. hematite, magnetite), **Pl:** plagioclase, **Q:** quartz, **Qs:** quartzite, **Sr:** sericite.

[b] **B:** basalt, **L:** limestone.

Table 2 shows the mineral/phases identified in the samples. As seen from the table quartz, plagioclase ($(Na,Ca)AlSi_3O_8$) and feldspars (K-feldspar ($KAlSi_3O_8$)) were the dominant phases while carbonates (mainly calcite) were generally the minor phases and occasionally major phases in some of the samples (S1 and S12). The simultaneous existence of the neoformations and calcite were furthermore assigned to probable appearance of secondary calcite which was also seen in the microphotographs of some samples (Fig. 3 and Fig. 4). Trace amounts of pyroxene and gehlenite minerals (for S5, S6, S7, S10 and S14) allowed us to assume that although such samples were fired up to the required temperature for the formation of new minerals, heating process did not exceed definitely the temperature threshold for the maturation. Besides, the presence of clay minerals (illite/muscovite) suggested a firing temperature not higher than 800-950 °C at which the structural decomposition of these raw materials is completed [7,8].

Hematite was identified in most of the samples pointing out that iron minerals were presumably the main coloring agents for the potsherds. Micro-Raman analysis of some selected representative samples also revealed the presence of iron minerals (i.e. hematite, magnetite) supporting the effect of these minerals in coloration (Fig. 5). In case of reducing atmosphere (absence of oxygen during the firing process) magnetite occurs resulting in dark shades while hematite causes the red, brown, and occasionally buff colors [9]. Having red-brown margin with black-gray core, the sandwich structured samples of S4, S5, S7, S8, S11 and S14 are believed to be subjected to both reducing and oxidative atmospheres during the firing process. Furthermore, as the outer layers of such samples are in reddish colors, it may be considered that the firing process of these samples has presumably ended in oxidative environment, but the oxidation did not reach the core of the bodies.

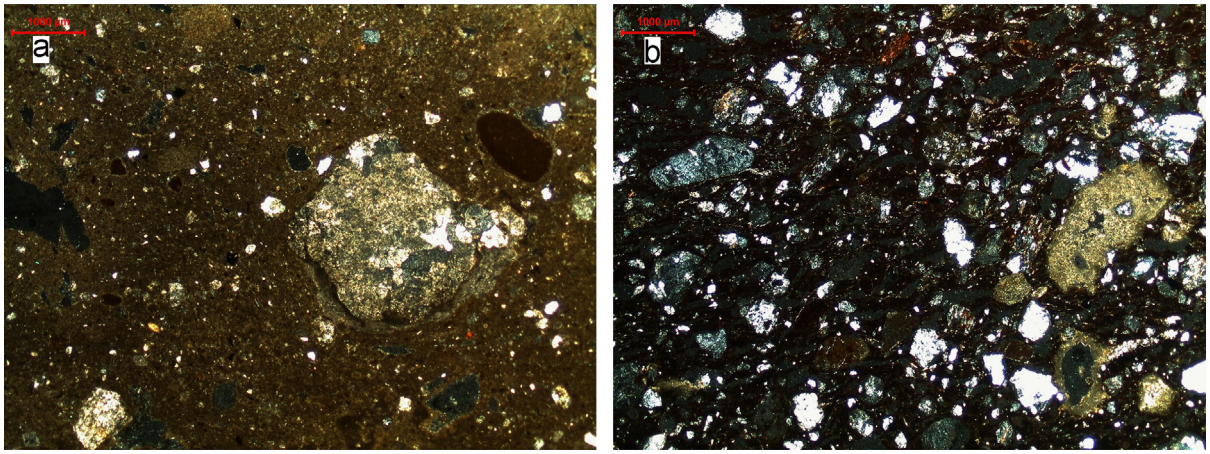


Fig. 3. (a) Grog fragment situated into the matrix (microphotograph of the sample of S11); (b) Inhomogeneous paste with high non-plastic material/matrix ratio (microphotograph of the sample of S5).

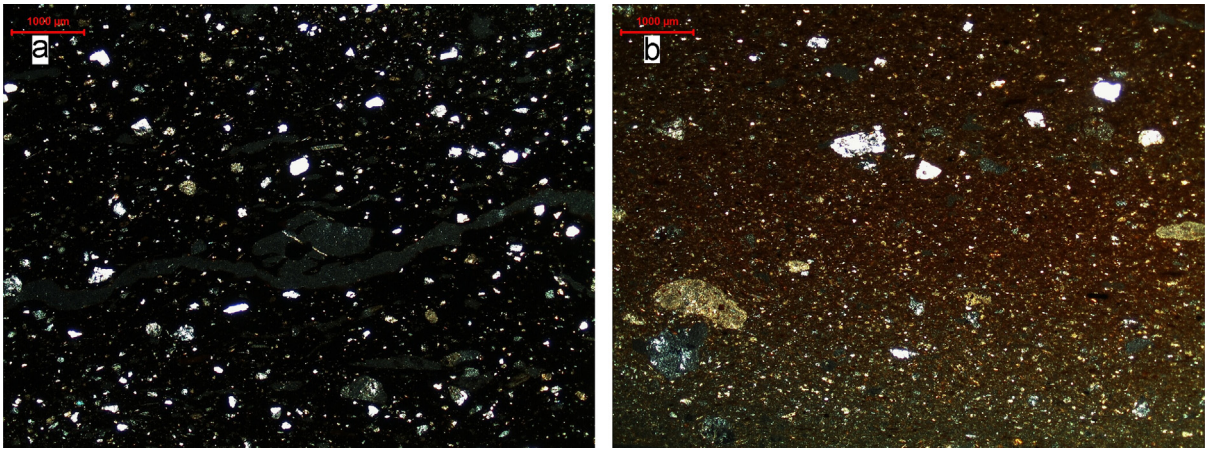


Fig. 4. (a) Microphotograph of the sample of S10 exhibits a matrix having relatively well-dispersed grains (containing probable secondary calcite formations with high birefringence) and also some salient traces demonstrating the gaps presumably occurred due to organic temper materials included in the initial raw materials; (b) Microphotograph of the sample of S2 shows the matrix with different shades of gray, red and brown probably indicating an uneven firing process and/or a poor raw material preparation (for interpretation of the references to color in this figure legend, the reader is referred to the web version of this article).

Table 2
XRD results.

Sample code	Mineral/phase							
	Q	Fs/Pl	Cc	I/M	Do	Pr	Gh	H
S1	***	*	*****	tr	****	–	–	–
S2	*****	**	tr	–	–	**	****	*
S3	*****	***	**	*	–	–	–	*
S4	*****	***	***	tr	–	–	–	*
S5	*****	**	tr	–	–	tr	tr	*
S6	*****	**	***	*	–	tr	tr	–
S7	*****	**	*	*	–	tr	tr	–
S8	*****	**	****	*	–	–	–	*
S9	*****	**	**	**	–	–	–	*
S10	*****	**	**	*	–	*	tr	*
S11	*****	**	***	*	–	–	–	*
S12	**	–	*****	*	–	–	–	–
S13	****	*	–	–	–	*****	–	–
S14	*****	**	**	tr	–	tr	*	–

*: Relative abundance, tr: trace amount. Q: quartz, Fs/Pl: feldspar/plagioclase, Cc: calcite, I/M: illite/muscovite, Do: dolomite, Pr: pyroxene (diopside/augite), Gh: gehlenite, H: hematite. The double, trible and four stars indicate to the abundance of the mineral/phase identified after the major ones in terms of their intensity (counts).

3.2. Thermogravimetric–differential thermal analysis (TG–DTA)

TG–DTA is one of the convenient methods preferred in characterization of ancient ceramics. This technique allows the examination of changes occurred due to the decomposition, transformation and formation reactions during a controlled heating process [10]. Samples were heated from room temperature to 1100 °C with a heating rate of 10 °C/min in order to expose the enthalpy changes (plotted by DTA curves with endothermic and exothermic effects) and weight loss/gain (plotted by TG curves). Characteristic enthalpy changes at specific temperature ranges are given in Table 3.

The endothermic effect from room temperature to 200 °C, which was identified in all of the samples, is due to the release of hygroscopic water [6]. At higher temperatures of 200–300 °C the endothermic effect depicts the removal of the chemically bound water, but not met in the present study [11]. Depending on the area of the peaks observed in the range of 200–650 °C, the exothermic effect identified within these temperatures was attributed to the combustion of organic materials, not completely burnt during firing in reducing condition and transformed into carbonaceous particles, which are thought to be deliberately added into the ceramic paste to increase its plasticity or were contained in the clay utilized in the manufacture [12,13].

The endothermic effects observed at 700–875 °C indicated the decarbonation reactions of mainly calcite and dolomite [13]. The highest endothermic effect at this range was seen on DTA curves of the samples of S1 and S12. Considering the XRD results of these two samples from Table 2, the presence of calcite and dolomite in the sample of S1 and the dominant existence of calcite along with lesser amounts of quartz and clay minerals in the sample of S12 were clearly confirmed by the DTA and TG curves of the samples (Figs. 6 and 7). The endothermic effect at this region was relatively low for the other samples. The lowest effect at the temperature range of decarbonation reactions was observed on DTA curves of the samples of S2, S5 and S13. Fig. 8 shows the TG–DTA curve of the sample of S2 in which the pyroxene and gehlenite were identified by XRD. These results allowed us to draw a conclusion that the weak endothermic effect, which is assigned to the removal of carbonated materials, may presumably be attributed to secondary calcite. This was also evidenced by the low abundance/intensity of calcite identified thorough the XRD results of some samples (S5, S7, S10 and S14). High temperature minerals (gehlenite and anorthite-pyroxene) and calcite were simultaneously identified for these samples and calcite was relatively low with respect to the primary calcite.

The formation of calcium silicates at higher temperatures (i.e. 850–950 °C) may be limited because of mainly three parameters; (i) grain size of calcite (coarse grains may expand the transition time/temperature), (ii) insufficient soaking time and peak temperature can bring incomplete transformation reactions, and (iii) the amount of calcite (large amounts of

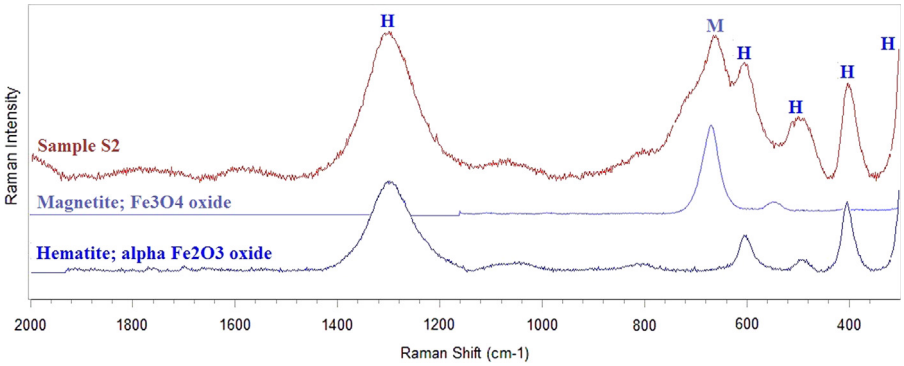


Fig. 5. Representative Raman spectrum of the sample of S2 (H: Hematite, M: Magnetite).

Table 3
TG–DTA results (enthalpy changes).

Sample code	Peak temperatures of enthalpy changes		
	Dehydration[a] (25–200 °C)	Decarbonatization[a] (700–875 °C)	Polymorphic transformation[a,b] (> 875 °C) and Sintering behavior[a,b] (> 1000 °C)
S1	83.7 °C (−0.079 μV/mg) 127.4 °C (−0.076 μV/mg)	772.5 °C (−0.361 μV/mg) 811.9 °C (−0.483 μV/mg)	1035.0 °C (−0.431 μV/mg) 1060.8 °C (−0456 μV/mg)
S2	83.4 °C (−0.027 μV/mg)	723.6 °C (−0.066 μV/mg)	1037.0 °C (−0.333 μV/mg) 1065.0 °C (−0.359 μV/mg)
S3	83.4 °C (−0.027 μV/mg)	753.0 °C (−0.118 μV/mg)	880.9 °C (−0.124 μV/mg) 1043.0 °C (−0.359 μV/mg) 1067.0 °C (−0.399 μV/mg)
S4	80.5 °C (−0.016 μV/mg)	765.2 °C (−0.155 μV/mg)	1049.0 °C (−0.371 μV/mg) 1073.0 °C (−0.406 μV/mg)
S5	82.7 °C (−0.026 μV/mg)	–	1050.9 °C (−0.414 μV/mg) 1079.0 °C (−0.439 μV/mg)
S6	85.5 °C (−0.031 μV/mg)	761.8 °C (−0.170 μV/mg)	1064.0 °C (−0.468 μV/mg)
S7	83.8 °C (−0.050 μV/mg) 142.7 °C (−0.052 μV/mg)	744.4 °C (−0.119 μV/mg)	890.1 °C (−0.166 μV/mg)
S8	90.3 °C (−0.215 μV/mg) 139.7 °C (−0.226 μV/mg)	800.3 °C (−0.112 μV/mg) 847.5 °C (−0.011 μV/mg)	–
S9	74.1 °C (−0.198 μV/mg)	750.6 °C (0.296 μV/mg)	876.8 °C (0.290 μV/mg) 1036.0 °C (−0.027 μV/mg) 1061 °C (−0.090 μV/mg)
S10	73.9 °C (−0.118 μV/mg)	776.8 °C (0.025 μV/mg)	1046 °C (−0.094 μV/mg) 1072.0 °C (−0.122 μV/mg)
S11	77.1 °C (−0.128 μV/mg)	798.9 °C (−0.015 μV/mg)	1043.0 °C (−0.079 μV/mg) 1068.0 °C (−0.103 μV/mg)
S12	78.6 °C (−0.145 μV/mg)	852.5 °C (−0.211 μV/mg)	1046.1 °C (−0.028 μV/mg) 1068.8 °C (−0.047 μV/mg)
S13	74.0 °C (−0.131 μV/mg)	719.0 °C (0.106 μV/mg)	1044.0 °C (−0.044 μV/mg)
S14	74.1 °C (−0.066 μV/mg)	742.0 °C (−0.007 μV/mg) 818.0 °C (−0.013 μV/mg)	1032.0 °C (−0.287 μV/mg) 1051.9 °C (−0.325 μV/mg)

-: not defined.
[a]Endothermic.
[b]Exothermic.

calcite may require higher temperature ranges along with a prolonged firing process) [14]. Thus, the minimum firing temperature range of such samples was considered as 800–850 °C. Finally, the negligible effects of endothermic and exothermic enthalpy changes observed above 875 °C and 1000 °C suggested that the polymorphic transformations and the sintering behavior were pretty low, respectively [3].

The values of weight loss/gain, which occur owing to the reactions of dehydration, decomposition of hydroxyls and decomposition of carbonated minerals, are the main stages in assessment process of TG curves [13]. The weight loss (Table 4) from room temperature to 200 °C, changing between 0.02 and 2.57%, was attributed to the removal of hygroscopic water and the weight loss at 400–600 °C, changing between 0.10 and 1.84%, was assigned to the decomposition of hydroxyls [10]. The hygroscopic water was assigned to burning of carbonaceous particles, if present, and loss of hydroxyls from rehydrated amorphous clay relicts during

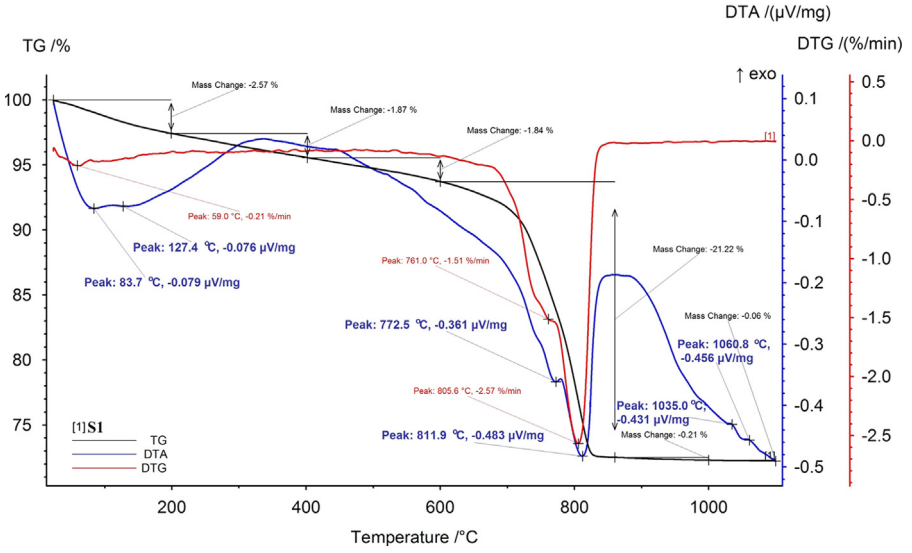


Fig. 6. TG–DTA curve of the sample of S1.

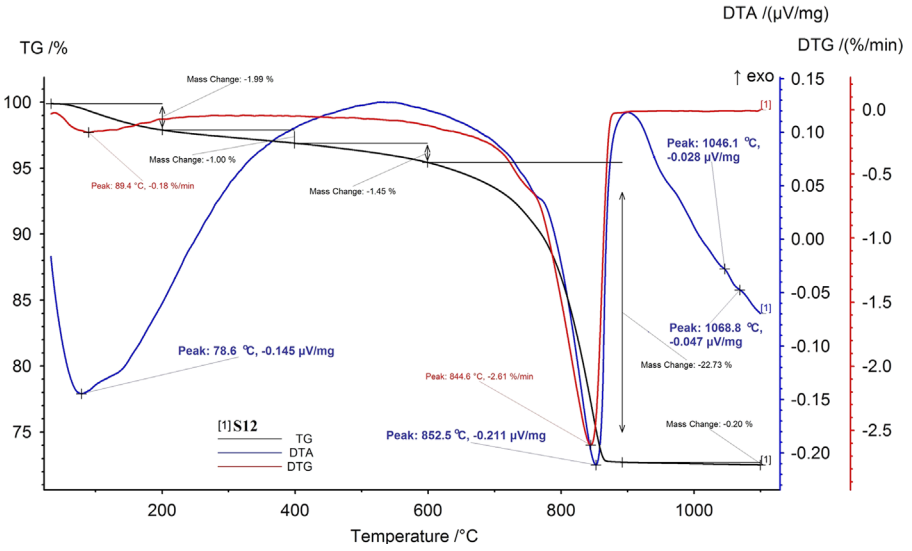


Fig. 7. TG–DTA curve of the sample of S12.

burial conditions (re-hydroxylation process). Also the hygroscopic water, loss at lower temperature, came from the humidity in the burial conditions.

The decomposition reaction of carbonates, which emerged at the temperature range of 600–850 °C, was identified with the weight losses changing between 0.56 and 22.73%. The existence of calcite–dolomite and the dominant presence of calcite in the samples of S1 and S12, respectively, were previously revealed by XRD (Table 2) and DTA (Fig. 6 and Fig. 7). These results showed that the sample of S1 was exposed to the lowest firing temperature (600–700 °C) due to the simultaneous existence of dolomite and calcite.

Considering the weight loss together with the enthalpy changes, it was concluded that the firing temperature of the samples changes from 600 °C to almost 950 °C. For some of the samples (i.e. S2, S5 and S13), the poor endothermic/exothermic effects supported with the low weight loss values belonging to the decarbonation reactions allowed us to predict that such potsherds presumably include calcite from re-carbonation process which might occur due to the burial conditions. For instance; when the free-lime contacts with the moisture it tends to form calcium hydroxide and this formation then reacts with CO_2 resulting in re-carbonated calcite [15]. Another possible way is the alteration of gehlenite that firstly generates calcium hydroxide which then reacts with CO_2 to form secondary calcite [14]. Secondary calcite can originate by precipitation from solution circulating in the burial soil.

3.3. SEM/EDS Results

Microchemical characteristics of the ceramics were studied in order to reveal the structural aspects which may vary mainly due to the raw materials and the firing conditions. With this aim, the representative samples of S1, S2, S6, S8, S12 and S13 were investigated using Zeiss Supra 50VP scanning electron

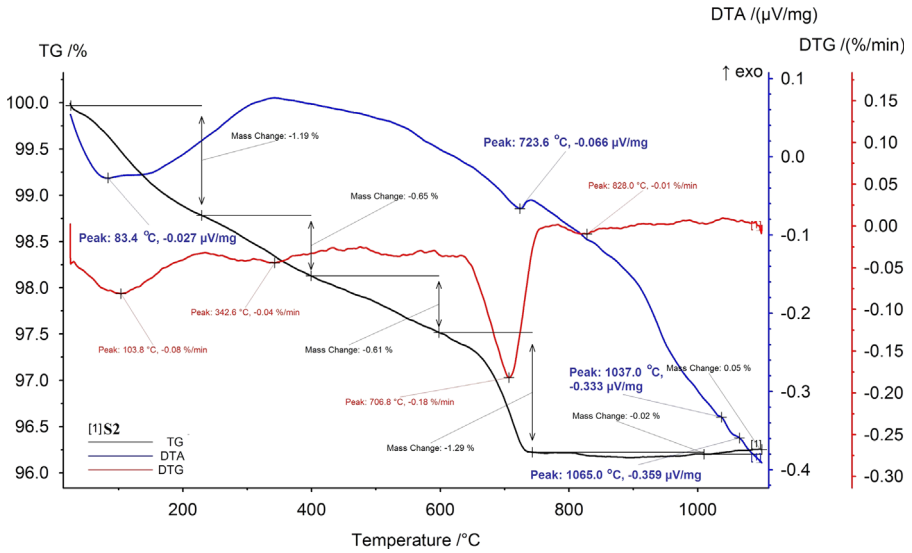


Fig. 8. TG–DTA curve of the sample of S2.

Table 4
TG–DTA results (weight loss per temperatures).

Sample code	Weight loss (wt. %)				
	Dehydration (25–200 °C)	Decomposition of hydroxyls (400–600 °C)	Decomposition of carbonated materials (600–850 °C)	Polymorphic transformation of crystalline or amorphous phases (> 850 °C)	Total (25–1100 °C)
S1	2.57	1.84	21.22	0.27	27.77
S2	1.19	0.61	1.29	0.02	3.76
S3	1.08	0.83	3.72	0.22	6.62
S4	0.78	0.42	3.63	0.45	5.68
S5	0.02	0.50	0.56	0.08	1.72
S6	0.88	0.65	4.20	0.09	6.52
S7	0.66	0.51	2.04	0.36	4.22
S8	2.13	1.17	6.86	0.16	11.71
S9	1.30	0.96	4.40	0.65	8.26
S10	0.58	0.63	4.05	0.29	6.06
S11	1.43	1.17	5.91	0.54	10.01
S12	1.99	1.45	22.73	0.20	27.37
S13	0.57	0.10	1.27	0.27	2.72
S14	0.56	0.44	2.66	0.22	4.24

microscopy equipped with the energy dispersive spectroscopy. Considering the mineral/phase contents of the potteries, the samples of S2 and S13 were selected owing to the obvious presence of new calcium silicates (gehlenite and anorthite-pyroxene, respectively) occurred at higher temperatures. From the back scattered electron (BSE) images of these samples (Fig. 9), a matrix with poor vitrification was observed. The absence of any smooth glassy structures and the presence of relatively coarse grains indicated a limited vitrification which probably occurred due to an uneven firing process (e.g. inadequate peak temperature, insufficient soaking time) along with a poor preparation process of raw materials (e.g. inhomogeneous grain distribution). The sample of S6 was chosen for it includes calcite, clay minerals and also high temperature minerals (in trace amounts) (Fig. 10). It was seen that this sample has preserved the laminar structure of the muscovite. The existence of this structure and also the high temperature minerals (in trace amounts) can be attributed to a firing temperature range of 800–850 °C at which new calcium silicates emerge and muscovite may persist.

The evident presence of carbonates was the main reason to study the samples of S1 and S8 which clearly include calcite-dolomite and calcite, respectively (Fig. 11). The BSE image of the sample of S1 indicated a ceramic paste with no vitrification and suggested a relatively low firing temperature. This prediction was also proved mainly with the presence of dolomite. An initial vitrification of sample S8 was observed in spite of the high calcite content. Finally, the sample of S12 was investigated due to the dominant existence of calcite. A relatively compact structure was seen from the BSE image of the sample of S12 (Fig. 12). This texture was also observed in the microphotograph of the same sample (Fig. 13).

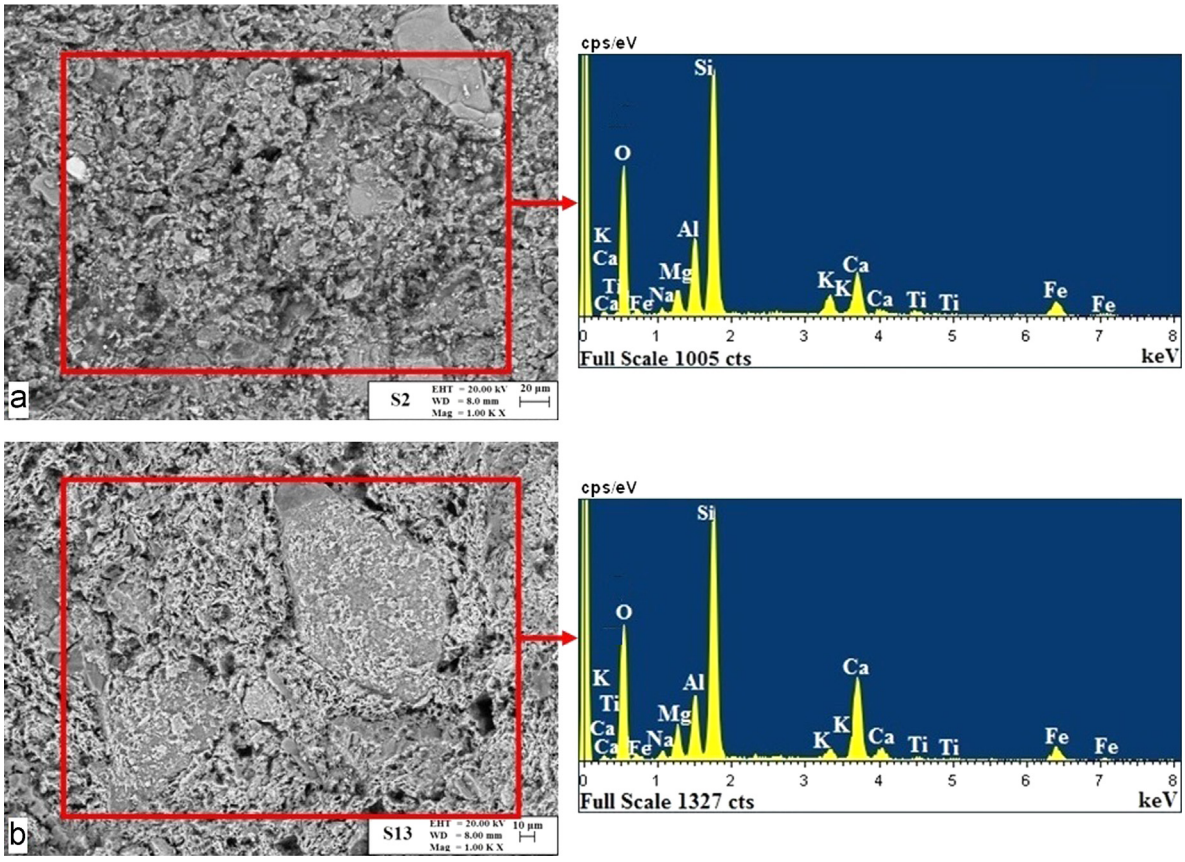


Fig. 9. Representative BSE images and EDS spectra of the samples of (a) S2 and (b) S13.

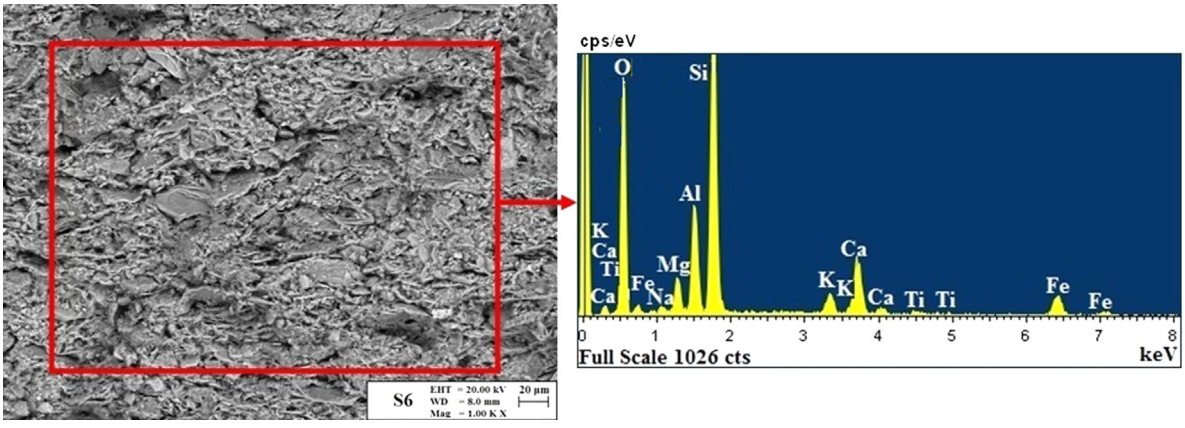


Fig. 10. Representative BSE image and EDS spectrum of the sample of S6.

4. Conclusions

The present study dealt with the characterization of the potsherds belonging to the First Millennium AD from the archeological site of Kuriki in southeastern Turkey. The mineralogical analyses suggested that the clay type used in manufacture of the potsherds was illitic, and slightly smectitic and kaolinitic for only few samples. The results of ceramic petrography analysis showed that basalt and limestone were the rock types which are thought to be the main sources for the minerals identified in the ceramic wares. Changing up to 58 vol%, the high total aggregate content of the samples suggested a poor raw material preparation process and also brought the question of probable use of aggregated minerals from the river bed formed at the intersection point of the Tigris River and the Batman Creek. The presence of grog fragments in some of the samples denoted that a recycling process may have been used by the potters in order to recover ceramic scraps and production rejects. The microphotographs of the representative samples showed that the samples may be

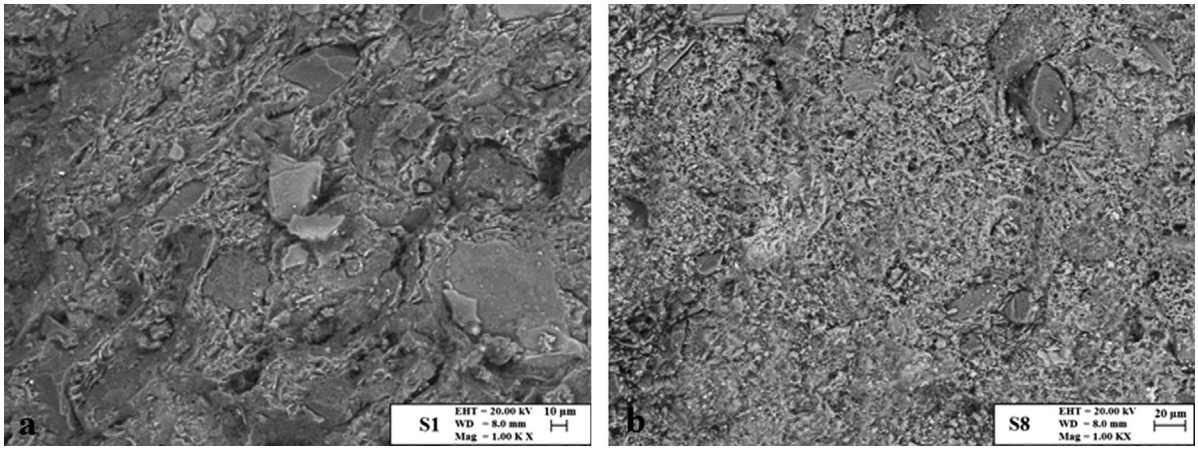


Fig. 11. Representative BSE images of the samples of (a) S1 and (b) S8.

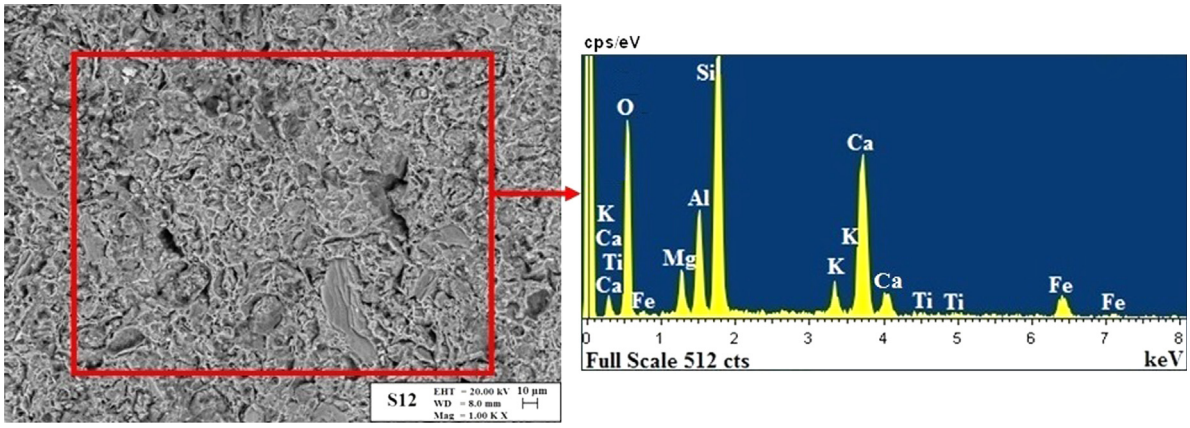


Fig. 12. Representative BSE image and EDS spectrum of the sample of S12.

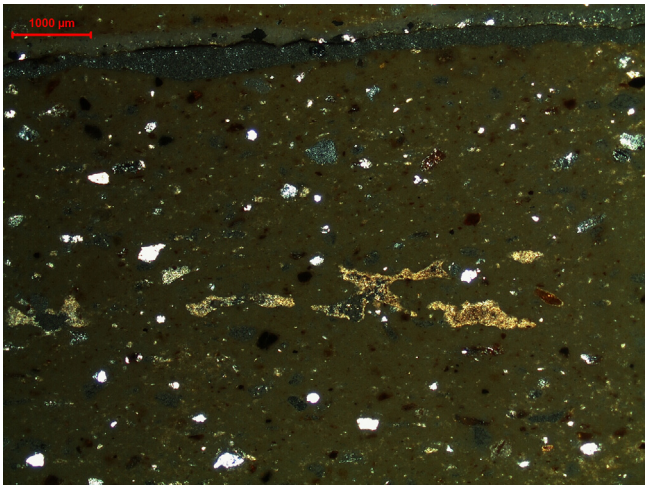


Fig. 13. Microphotograph of the sample of S12.

classified into two groups due to the size and distribution of the grains forming the paste; i: inhomogeneous paste with high non-plastic material/matrix ratio and with relatively coarse grains, ii: consisted of relatively fine grains well-dispersed into the matrix. This may allow us to draw a conclusion that the ceramics were presumably produced in two different ways depending on may be the purpose of use.

According to the XRD results quartz, plagioclase and feldspars were found as the dominant phases. Carbonates were found as the minor phases and occasionally as major phases in some of the samples. Hematite was identified in most of the samples indicating that the iron minerals were the natural coloring agents of the potsherd bodies. It was also concluded that the sandwich structured samples with red-brown margin and black-gray core have probably undergone both reducing and oxidative atmospheres during the firing process. The exterior colors of reddish and brownish observed in some samples suggested a firing process which has ended in an oxidative environment. While the evident presence of gehlenite and anorthite-pyroxene suggested a minimum firing temperature of 850–900 °C, the absence or scarce occurrence of these minerals in some of the samples indicated an incomplete firing process with insufficient soaking time required for the maturation of the ceramics. SEM/EDS analysis confirmed the results of the diffractometric and thermal analyses. From the back scattered electron (BSE) images of such samples it was seen that most of the potsherds have been subjected to firing temperatures not higher than 950 °C due to relatively low vitrification degree.

Carbonates (calcite and dolomite) were well identified by TG and DTA curves. The poor effects observed in temperature range of decarbonation in some samples, fired at relatively

high temperature, were thought to be the formation of secondary calcite and were attributed to the burial conditions. The results of this study are believed to provide a convenient knowledge for the ceramic production in the region of south-eastern Turkey (Upper Mesopotamia) and also to ensure a basis for the researchers to have collaborative and comparative investigations.

Acknowledgments

The Scientific Research Projects (BAP) department of Batman University (Turkey) is greatly acknowledged for the financial support (Project number: BTUBAP-2011-GSF-3).

References

[1] G. Eramo, R. Laviano, I.M. Muntoni, G. Volpe, Late Roman cooking pottery from the Tavoliere area (Southern Italy): raw materials and technological aspects, J. Cult. Herit. 5 (2004) 157–165.

[2] S. Charters, R.P. Evershed, L.J. Goad, C. Heron, P. Blinkhorn, Identification of an adhesive used to repair jar, Archaeometry 35 (1993) 91–101.

[3] A. Krapukaitytė, S. Tautkus, A. Kareiva, E. Zalieckienė, Thermal analysis—a powerful tool for the characterization of pottery, Chemija 19 (2008) 4–8.

[4] S.R. Bertolino, V.G. Josa, A.C. Carreras, A. Laguens, G. De La Fuente, J.A. Riveros, X-ray techniques applied to surface paintings of ceramic pottery pieces from Aguada Culture (Catamarca, Argentina), X-Ray Spectrom. 38 (2009) 95–102.

[5] A. Issi, Estimation of ancient firing technique by the characterization of semi-fused Hellenistic potsherds from Harabebezikan/Turkey, Ceram. Int. 38 (2012) 2375–2380.

[6] L. Maritan, L. Nodari, C. Mazzoli, A. Milano, U. Russo, Influence of firing conditions on ceramic products: experimental study on clay rich in organic matter, Appl. Clay Sci. 31 (2006) 1–15.

[7] G. Cultrone, C. Rodriguez-Navarro, E. Sebastian, O. Cazalla, M.J. De La Torre, Carbonate and silicate phase reactions during ceramic firing, Eur. J. Mineral. 13 (2001) 621–634.

[8] A. Iordanidis, J. Garcia-Guinea, G. Karamitrou-Mentessidi, Analytical study of ancient pottery from the archeological site of Aiani, northern Greece, Mater. Charact. 60 (2009) 292–302.

[9] A. Issi, A. Raškovska, A. Kara, O. Grupce, B. Minčeva-Šukarova, F. Okyar, Scanning electron microscopy and micro-Raman spectroscopy of slip layers of Hellenistic ceramic wares from Dorylaion/Turkey, Ceram. Int. 37 (2011) 1879–1887.

[10] V.A. Drebushchak, L.N. Mylnikova, T.N. Drebushchak, V.V. Boldyrev, The investigations of ancient pottery, J. Therm. Anal. Calorim. 82 (2005) 617–626.

[11] L. Paama, I. Pitkanen, P. Peramaki, Analysis of archeological samples and local clays using ICP-AES, TGDTG and FTIR techniques, Talanta 51 (2000) 349–357.

[12] R. Palanivel, U. Rajesh Kumar, Thermal and spectroscopic analysis of ancient potteries, Rom. J. Phys. 56 (2011) 195–208.

[13] S. Meyvel, P. Sathya, G. Velraj, Thermal characterization of archeological pot sherds recently excavated in Nedunkur, Tamilnadu, India, Cerâmica 58 (2012) 338–341.

[14] B. Fabbri, S. Gualtieri, S. Shoval, The presence of calcite in archeological ceramics, J. Eur. Ceram. Soc. 34 (2014) 1899–1911.

[15] S. Shoval, M. Gaft, P. Beck, Y. Kirsh, The thermal behavior of limestone andmonocrystalline calcite tempers during firing and their use in ancient vessels, J. Therm. Anal. 40 (1993) 263–273.